Indian Geotechnical Journal, Vol. 23 (4), 1993

Stability of Slopes in Partially Saturated Soils

by

A. Siva Reddy*

Alok Agarwal**

Introduction

Many of the natural soils in tropical countries are partly saturated. Embankments constructed by compacting soils at or close to optimum moisture content are also partly saturated. In cases like this, the pore water pressure in soil is negative. Porewater pressures, as low as -46.7 t/m^2 at optimum water content and as low as —166.7 t/m^2 at 5 percent dry optimum (Oslon and Langfelder, 1965). Mogalaih and Ranganatham (1972) have measured —13.3 t/m^2 of pore pressure in compacted kaolinite. It is well known that vast areas on the surface of the earth are classified as arid or semiarid regions where soils are in unsaturated state. Some researchers (Low, 1967) argue that negative pore water pressure should not be relied upon in the stability analysis of slopes. However, one may wonder, to what extent the strength of soil, imparted to it by suction, is being neglected if the partial saturation is not accounted for. The possibility of using this strength in design should be explored. This paper presents the analysis of stability of slopes in unsturated soils using a new approach developed in the method of characteristics.

Of the various methods of analysis for investigating the stability of earth embankments and cuttings, limit equilibrium methods are the ones mostly used. These methods are associated with a series of assumptions regarding the failure surfaces and position and direction of forces acting. Trial and error method is adopted for the identification of the failure surface which gives minimum value of factor of safety. However, as this trial procedure does not cover all the possible slip surfaces it is obvious that other surfaces could lead to different values of factor of safety . Also, the problem being an indeterminate one, all the equations of equilibrium are not satisfied. In the method of characteristics all these shortcomings can be overcome.

Using the method of characteristics, Sokolovsky (1960) determined critical shape of a slope for a factor of safety of one. The horizontal

*Professor
**Formerly Research Scholar
} Department of Civil Engineering, Indian Institute of Science, Bangalore 560 012, India.

top of the slope was subjected to a loading. He assumed the soil to be homogeneous and isotropic and at failure at each and every point of which the last one is not physically possible. In the analysis presented here this assumption has been removed. Also the method of characteristics is further developed for straight slopes.

It is assumed here that u_o is the initial negative pore water pressure when the soil is at equilibrium under the action of initial stresses. As the embankment is made, there will be a change in the pore water pressure. Using Skempton's (1954) pore water pressure parameters this change is analysed and final pore water pressure is arrived at. From the Mohr-Coulomb failure criterion and the equations of equilibrium, equations along the two characteristics lines are derived. Along one of these, mobilized angle of internal friction is taken to be constant and the path of this is arrived at. Thus using finite difference technique the contours of mobilized angle of internal friction are obtained. No assumption regarding failure surfaces is made. All equations of equilibrium are satisfied. Taylor's definition of factor of safety has been used in the analysis.

Formulation of Problem and Derivation of Equations

Figure 1 shows a schematic diagram of the problem. As the slope is made of soil, it is subjected to stresses that cause a change in the pore water pressure. Due to the construction of the embankment the pore water pressure changes from initial u_o to u. The expression for final pore water pressure, u, at any point z below the horizontal top, as given by Reddy and Mogaliah (1970) is as follows

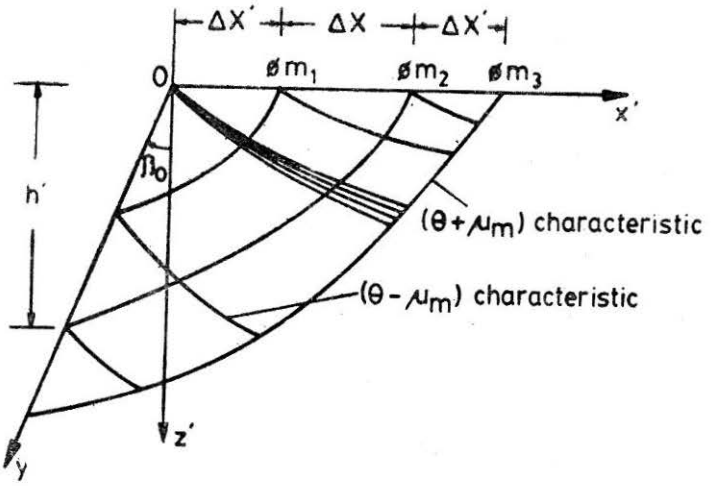

FIGURE 1 Definition sketch

$$u = \frac{B}{1-B}\left[\ \sigma\left\{1+(2A-1)\sin\phi_m\right\} - H + \gamma z\,(A\,k_o - A - k_o) + u_o\,(k_o - 1)\,(1-B) + \frac{u_o}{B}\right] \tag{1}$$

where **u** and H are as defined in Fig. 2. $u = 0$, when $A = B = u_o = 0$. Fig. 3 shows a soil element at equilibrium under the action of various forces. Considering the equilibrium of the element, the following two equations of equilibrium can be obtained.

$$\frac{\partial \sigma_x}{\partial x} + \frac{\partial u}{\partial x} + \frac{\partial \tau_{xz}}{\partial z} = \bar{x} \tag{2}$$

$$\frac{\partial \sigma_z}{\partial z} + \frac{\partial u}{\partial z} + \frac{\partial \tau_{xz}}{\partial x} = \bar{z} \tag{3}$$

where σ_x and σ_z are effective stresses

$\bar{x}$ and $\bar{z}$ = body forces per unit volume in x and z directions, respectively,

$\bar{x} = 0$ and $\bar{z} = \gamma$ where γ is specific weight of the soil.

The following assumptions are made in the analysis

(*i*) The problem is two dimensional

(*ii*) Mohr-Coulomb's failure criterion is valid for the soil

(*iii*) Soil mass is rigid plastic at failure.

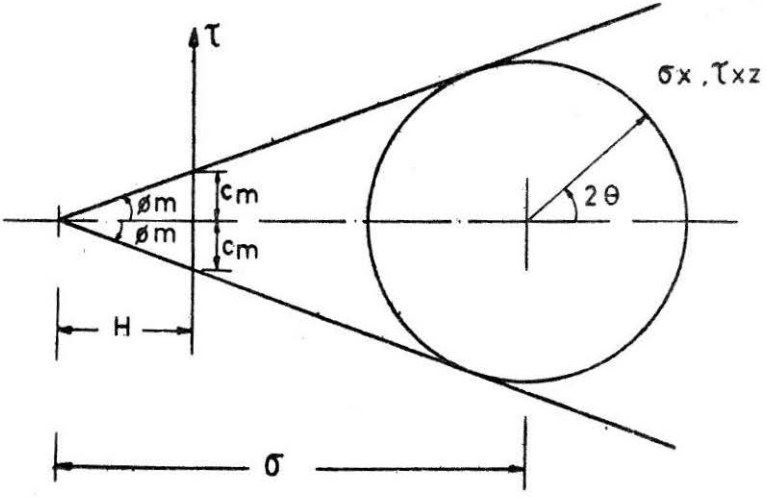

FIGURE 2 Mohr's circle showing state of stress at a point

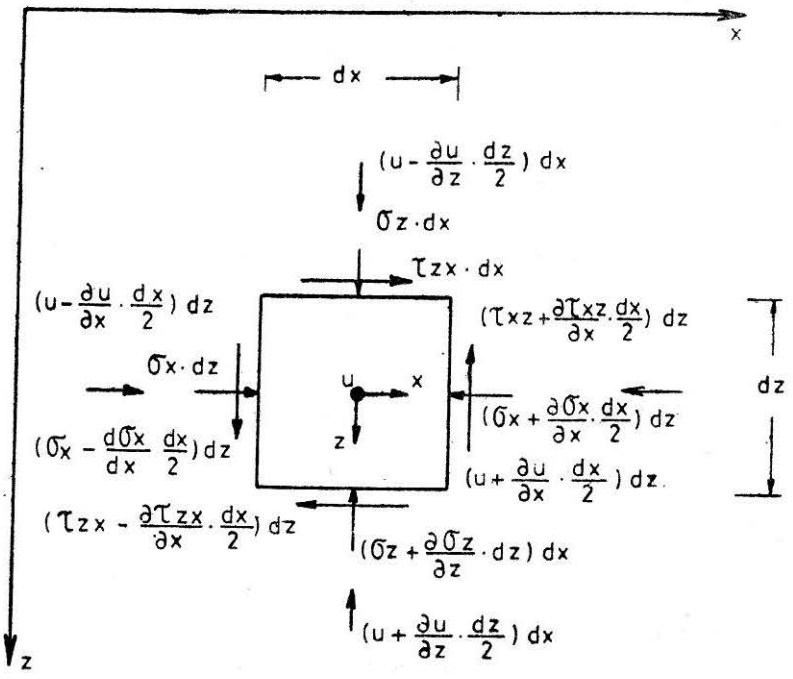

FIGURE 3 Soil element in equilibrium under the stresses shown

The angle of internal friction mobilised is taken as a function of cartesian co-ordinates. The equations along the characteristics, from which ϕ_m contours are obtained, are derived in terms of σ and θ. Defining factor of safety, F, as

$$F = \frac{c}{c_m} = \frac{\tan\phi}{\tan\phi_m} = \frac{c+\sigma_n \tan\phi}{c_m+\sigma_n\tan\phi_m},$$

from Fig. 2, it can be seen that

$$H = c.\ \cot\phi = c_m.\cot\phi_m = \text{constant}$$

Also, σ_x, σ_z and τ_{xz} are given by the following expressions.

$$\left.\begin{matrix}\sigma_x\\ \sigma_z\end{matrix}\right\} = \sigma(1 \pm \sin\phi_m.\cos 2\theta) - H \qquad (4)$$

$$\tau_{xz} = \sigma.\sin\phi_m.\sin 2\theta \qquad (5)$$

Substituting equations (1), (4) and (5) in equations (2) and (3), and simplifying, the following equations are obtained.

$$(1+M+\sin\phi_m\cos2\theta).\ \frac{\partial\sigma}{\partial x}+\sigma\cos\phi_m\left\{\frac{B(2A-1)}{(1-B)}\frac{\partial\phi_m}{\partial x}+\cos\theta\frac{\partial\phi_m}{\partial x}+\sin2\theta\frac{\partial\phi_m}{\partial z}\right\}-2\sigma\sin\phi_m\left\{\sin2\theta\frac{\partial\theta}{\partial x}-\cos2\theta.\frac{\partial\theta}{\partial z}\right\}+\sin\phi_m.\sin2\theta.\frac{\partial\sigma}{\partial z}=0 \tag{6}$$

$$(1+M-\sin\phi_m.\cos2\theta)\frac{\partial\sigma}{\partial z}+\sigma\cos\phi_m\left\{\frac{B(2A-1)}{(1-B)}.\frac{\partial\phi_m}{\partial z}-\cos2\theta.\frac{\partial\phi_m}{\partial z}+\sin2\theta.\frac{\partial\phi_m}{\partial x}\right\}+2\sigma\sin\phi_m\left\{\sin2\theta.\frac{\partial\theta}{\partial z}+\cos2\theta.\frac{\partial\theta}{\partial x}\right\}+\sin\phi_m.\sin2\theta.\frac{\partial\sigma}{\partial x}=N \tag{7}$$

where

$$M=\frac{B}{1-B}\left\{1+(2A-1).\sin\phi_m\right\} \tag{8}$$

$$N=\gamma\left\{1-\frac{B}{1-B}(A.K_o-AK_o)\right\} \tag{9}$$

when there is no pore water pressure and ϕ_m is a constant the above equations reduce to Sokolovsky equations.

Multiplying equation (6) by sin $(\theta\pm\mu_m)$ and equation (7) by —cos $(\theta\pm\mu_m)$, adding the resulting equations and simplifying, the following expressions are obtained.

$$\{1+M\pm M.\tan\phi_m.\tan(\theta\mp\mu_m)\}.\frac{\partial\sigma}{\partial x}+(1+M).\tan(\theta\mp\mu_m)\frac{\partial\sigma}{\partial z}\pm M\tan\phi_m\frac{\partial\sigma}{\partial z}\pm\frac{\sigma.\partial\phi_m/\partial x}{\cos(\theta\mp\mu_m)}.\{Q.\sin(\theta\pm\mu_m)-\sin(\theta\mp\mu_m)\}\pm\frac{\sigma.\partial\phi_m/\partial z}{\cos(\theta\mp\mu_m)}.\{\cos(\theta\mp\mu_m)-Q.\cos(\theta\pm\mu_m)\}\mp2\sigma\tan\phi_m\frac{\partial\theta}{\partial x}\mp2\sigma\tan\phi_m\tan(\theta\mp\mu_m)\frac{\partial\theta}{\partial z}=\mp\frac{N\cos(\theta\mp\mu_m)}{\cos\phi_m\cos(\theta\mp\mu_m)} \tag{10}$$

where $Q=\dfrac{B(2A-1)}{(1-B)}$

and $\mu_m=\dfrac{\pi}{4}-\dfrac{\phi_m}{2}$

At any point on a plane where the angle of internal friction mobilized is ϕ_m, the planes make equal angle $\pm\mu_m$ with the direction of the major principal stress.

Introducing auxiliary variables P_a and Q_a given by the following expressions

$$P_a = (1+M).\ \frac{\partial \sigma}{\partial x} \pm M.\tan\phi_m \tan(\theta \mp \mu_m).\ \frac{\partial \sigma}{\partial x} \mp 2\tan\phi_m\ \frac{\partial \theta}{\partial x} \pm \frac{\sigma\, \partial\phi_m/\partial x}{\cos(\theta \mp \mu_m)}$$

$$\{Q\sin(\theta \pm \mu_m) - \sin(\theta \mp \mu_m)\} \pm \frac{\sigma.\partial\phi_m/\partial z}{\cos(\theta \mp \mu_m)} \cdot \{\cos(\theta \mp \mu_m) - Q.\cos$$

$$(\theta \pm \mu_m)\} \pm \frac{N.\cos(\theta \pm \mu_m)}{\cos\phi_m.\cos(\theta \mp \mu_m)} \qquad (11)$$

and

$$Q_a = (1+M)\ \frac{\partial \sigma}{\partial z} \mp M\tan\phi_m \cot(\theta \mp \mu_m)\ \frac{\partial \sigma}{\partial z} \mp 2\sigma\tan\phi_m\ \frac{\partial \theta}{\partial z} \qquad (12)$$

The generalized equation (10) can be rewritten as

$$P_a + Q_a.\tan(\theta \mp \mu_m) = 0 \qquad (13)$$

transforming the previous equations in the following way

$$P_a + Q_a.\ \frac{dz}{dx} = R_a$$

or

$$P_a\, dx + Q_a\, dz = R_a.\, dx \qquad \text{and} \qquad (14)$$

solving equations (13) and (14) for P_a and Q_a

$$Q_a = -\ \frac{R_a.\mathrm{dx}.\cos(\theta \pm \mu_m)}{\sin(\theta \mp \mu_m)\ \mathrm{dx} - \cos(\theta \mp \mu_m)\mathrm{dz}} \qquad (15)$$

$$P_a = \frac{R_a\ \mathrm{dx}\ \sin(\theta \mp \mu_m)}{\sin(\theta \mp \mu_m)\ \mathrm{dx} - \cos(\theta \mp \mu_m)\ \mathrm{dz}} \qquad (16)$$

Further, the expressions for the total differentials for σ and θ are given by

$$d\sigma = \frac{\partial \sigma}{\partial x} \cdot \mathrm{dx} + \frac{\partial \sigma}{\partial z} \cdot \mathrm{dz} \qquad (17)$$

$$d\theta = \frac{\partial \theta}{\partial x} \cdot \mathrm{dx} + \frac{\partial \theta}{\partial z} \cdot \mathrm{dz} \qquad (18)$$

Substituting from equations (11) and (12) for P_a and Q_a in equation (14), using equations (17) and (18) and equating to zero simultaneously the numerators and denominators of equations (15) and (16) the following relationships are obtained.

$$\frac{dz}{dx} = \tan(\theta \mp \mu_m) \qquad (19)$$

and

$$\{1+M\mp M\tan\phi_m\cot(\theta\mp\mu_m)\}\,d\sigma\mp 2\sigma\tan\phi_m\,d\theta\pm M\tan\phi_m\frac{\partial\sigma}{\partial x}\,dx'$$

$$.\{\tan(\theta\mp\mu_m)+\cot(\theta\mp\mu_m)\}=\mp\frac{N\cos(\theta\pm\mu_m)}{\cos\phi_m\cos(\theta\mp\mu_m)}dx$$

$$\mp\frac{\sigma.\partial\phi_m/\partial x}{\cos(\theta\mp\mu_m)}.\{Q.\sin(\theta\pm\mu_m)-\sin(\theta\mp\mu_m)\}\,dx$$

$$\mp\frac{\sigma.\partial\phi_m/\partial z}{\cos(\theta\mp\mu_m)}.\{\cos(\theta\mp\mu_m)-Q.\cos(\theta\pm\mu_m)\}\,dx \qquad (20)$$

In equations (19), the family of lines corresponding to the upper sign are called the $(\theta-\mu_m)$ characteristics, and those of the lower sign are called the $(\theta+\mu_m)$ characteristics. In equations (20) the equation corresponding to the upper sign holds along the $(\theta-\mu_m)$ characteristics while that corresponding to the lower sign holds along the $(\theta+\mu_m)$ characteristics.

For the non-dimensionalization, H, which has the dimension of stress and is a constant, is chosen as characteristic stress. Defining characteristic length, l, as H/γ, the following non-dimensional quantities (primed quantities) can be obtained.

$$\sigma'=\sigma/H,\ x'=x/l \text{ and } z'=z/l$$

Using these definitions, equations (19) and (20) can be written in non-dimensional form as

$$\frac{dz'}{dx'}=\tan(\theta\mp\mu_m) \qquad (21)$$

and

$$\{1+M\mp M.\tan\phi_m\cot(\theta\mp\mu)\}\,d\sigma'\mp 2\sigma'\tan\phi_m\,d\theta\pm M\tan\phi_m\frac{\partial\sigma'}{\partial x'}\,dx'$$

$$.\{\tan\theta\mp\mu_m)+\cot(\theta\mp\mu_m)\}=\mp\frac{N'\cos(\theta\pm\mu_m)}{\cos\phi_m\cos(\theta\mp\mu_m)}dx'$$

$$\mp\frac{\sigma'.\partial\phi_m/\partial x'}{\cos(\theta\mp\mu_m)}.(Q.\sin(\theta\pm\mu_m)-\sin(\theta\mp\mu_m))\,dx'$$

$$\mp\frac{\sigma'.\partial\phi_m/\partial z'}{\cos(\theta\mp\mu_m)}.\{Q.\sin(\theta\mp\mu_m)-Q.\cos(\theta\pm\mu_m)\}\,dx' \qquad (22)$$

where

$$N'=1-\frac{B}{(1-B)}.(AK_o-A-K_o)$$

Boundary Conditions

(*i*) Solution at the boundary ox (see Fig. 1)

Putting $z = 0$ in equation (1) the final pore water pressure, after the slope has been made is obtained as,

$$u_{z=o} = U1\sigma - U2H + \{U2(K_o-1)(1-A) + U2/B\}\, u_o$$

where $U1 = M$ and $U2 = \dfrac{B}{1-B}$

From equation (4), the condition along ox can be written as

σ_z = effective stress in z—direction

= total stress $-u$ $= o-u$

or

$$-u_{z=0} = \sigma\,(1-\sin\phi_m.\cos 2\theta) - H$$

whence, σ along ox, i.e, σ_{ox} can be obtained as

$$\sigma_{ox} = \frac{(1+U2)H - \{U2(K_o-1)(1-A) + U2/B\}\, u_o}{(1+U1+\sin\phi_m)}$$

Dividing by H for non-dimensionalizing

$$\sigma_{ox}/H = \sigma'_{ox} = \frac{(1+U2 - \{U2(K_o-1)(1-A) + U2/B\}\, u_o/H}{(1+U1+\sin\phi_m)} \qquad (23)$$

Here u_o/H represents the non-dimensional value of the negative pore water pressure.

Also as along ox soil is in active state, normal direction to ox is the direction of the major principle stress.

Therefore, θ along ox, i.e. $\theta_{ox} = \pi/2$ (24)

(ii) Solution at the singular point

As the soil along OA moves along the slope and is in active state the value of $\theta_{OA} = \pi/2 + \beta_o$. Therefore, at point '0' there is a sudden change in the angle θ from left of it to the right. This change is made gradual by introducing a number of $(\theta - \mu_m)$ lines at the point. As at this point $(\theta + \mu_m)$ line shrinks to a point, substituting $dx' = 0$ and $dz' = 0$ in the equation valid along $(\theta + \mu_m)$ characteristic, we obtain

$$(1+M)\, d\sigma'.2\sigma' \tan\phi_m.d\theta = 0$$

This on integration and evaluation of constant by applying condition along ox gives the following expression for the calculation of σ' for different values of θ at the singular point.

$$\sigma' = \sigma'_{ox}.\ \mathrm{EXP}\left[\frac{2.\tan\phi_m\,(\theta_{ox}-\theta)}{(1+M)}\right] \qquad (25)$$

(iii) Solution at the intersection of two characteristics

Knowing the values of σ', θ, x' and z' at the boundary ox these values at the intersection of two characteristics can be found using finite difference technique. Expressing equations (21) in the forward difference form and solving for the coordinates of the point of intersection x_3' and z_3', the following expressions are obtained

$$x_3' = \frac{z_2'-z_1'+x_1' \tan(\theta_1-\mu_{m1})-x_2' \tan(\theta_2+\mu_{m2})}{\tan(\theta_1-\mu_{m1})-\tan(\theta_2+\mu_{m2})} \tag{26}$$

and

$$z_3' = z_1'+(x_3'-x_1').\tan(\theta_1-\mu_{m1}) \tag{27}$$

where

$$\mu_{m1}= \pi/4-\phi_{m1}/2 \text{ and } \mu_{m2} = \pi/4-\phi_{m2}/2$$

Similarly, the equation along $(\theta-\mu_m)$ line can be written as

$$R1\ (\sigma_3'-\sigma_1') - (\sigma_3' + \sigma_1') + R2.\theta_3 + (\sigma_3' + \sigma_1').R2.\theta_1 + R_3 = -R4-R(\sigma_3' + \sigma_1') \tag{28}$$

where

$M1 = U2\{1 + (2A-1)\sin\phi_{m1}\}$; $M2 = U2\{1 + (2A-1).\sin\phi_{m2}\}$

$M3 = (M1+M2)/2$

$$R1 = 1 + M3-M3.\ \frac{\tan\phi_{m3} + \tan\phi_{m1}}{2} \cdot \frac{x_3'-x_1'}{z_3'-z_1'}$$

$$R2 = \frac{\tan\phi_{m3} + \tan\phi_{m1}}{2}$$

$$R3 = M3.\ \frac{\tan\phi_{m3}+\tan\phi_{m1}}{2} \cdot (x_3'-x_1').\left\{\frac{z_3'-z_1'}{x_3'-x_1'} + \frac{x_3'-x_1'}{z_3'-z_1'}\right\} \cdot \left(\frac{\partial\sigma'}{\partial x'}\right)_1$$

$$R4 = \frac{2N'}{\cos\phi_{m3}+\cos\phi_{m1}} \cdot \left\{(x_3'-x_1').\ \frac{\sin\phi_{m3}+\sin\phi_{m1}}{2} - (z_3'-z_1').\ \frac{\cos\phi_{m3} + \cos\phi_{m1}}{2}\right\}$$

$$R5 = [Q.\left\{(z_3'-z_2').\ \frac{\sin\phi_{m3}+\sin\phi_{m1}}{2} + (x_3'-x_1')\ \frac{\cos\phi_{m3}+\cos\phi_{m1}}{2}\right\} -(z_3'-z_1')]. \left(\frac{\partial\phi_m}{\partial x'}\right)_3 . \tfrac{1}{2}$$

$$R6 =\left[(x_3'-x_1')-Q.\left\{(x_3'-x_1').\ \frac{\sin\phi_{m3}+\sin\phi_{m1}}{2}-(z_3'-z_1').\ \frac{\cos\phi_{m3}+\cos\phi_{m2}}{2}\right\}\right]. \left(\frac{\partial\phi_m}{\partial z'}\right)_3 . \tfrac{1}{2}$$

and

$R = R5 + R6$; $\left(\frac{\partial \phi_m}{\partial x'}\right)_a$ = partial derivative of ϕ at point 3. The equation along $(\theta + \mu_m)$ characteristic, for which $\phi_{m3} = \phi_{m2}'$ can be expressed in the following way

$$S1\,(\sigma_3' - \sigma_2') + S2(\sigma_3' + \sigma_2')\,\theta_3 - S2\,(\sigma_3' + \sigma_2')\,\theta_2 - S3 = S4 + S(\sigma_3' + \sigma_2') \quad (29)$$

where

$$M3 = U2.\,\{1 + (2A - 1).\sin\phi_{m2}\}$$

$$S1 = 1 + M3 + M3.\tan\phi_{m2}.\ \frac{x_3' - x_2'}{z_3' - z_2'}$$

$$S2 = \tan\phi_{m2}$$

$$S3 = M3.\tan\phi_{m2}.\,(x_3' - x_2')\,.\left\{\frac{z_3' - z_2'}{x_3' - x_2'} + \frac{x_3' - x_2'}{z_3' - z_2'}\right\}.\left(\frac{\partial \sigma'}{\partial x'}\right)_2$$

$$S4 = \frac{N'}{\cos\phi_{m2}}\left\{(x_3' - x_2').\sin\phi_{m2} + (z_3' - z_2').\cos\phi_{m2}\right\}$$

$$S5 = [Q.\,\{(z_3' - z_2').\,\sin\phi_{m2} - (x_3' - x_2')\,\cos\phi_{m2}\} - (z_3' - z_2')].\left(\frac{\partial \phi_m}{\partial x'}\right).\frac{1}{2}$$

$$S6 = [(x_3' - x_2') - Q\,\{(x_3' - x_2').\,\sin\phi_{m2} + (z_3' - z_2').\,\cos\phi_{m2}\}).\left(\frac{\partial \phi_m}{\partial z'}\right).\frac{1}{2}$$

and

$$S = S5 + S6$$

From equations (28) and (29) the expressions for σ_3' can be obtained as

$$\sigma_3' = \frac{R8 - R2.\theta_3.\sigma_1'}{\theta_3.R2 - R7} = \frac{S8 - S2.\theta_3.\sigma_2'}{\theta_3.S2 - S7} \quad (30)$$

where

$$R7 = R1 + R2.\theta_1 + R$$

$$S7 = S1 + S2.\theta_2 + S$$

$$R8 = -R1.\sigma_1' + R2.\theta_1.\sigma_1' + R3 + R4 + R.\sigma_1'$$

$$S8 = -S1.\sigma_2' + S2.\theta_2.\sigma_2' + S3 + S4 + S.\,\sigma_2'$$

From equations (30) the following expression for θ_3 is obtained

$$\theta_3 = \frac{-B3 \pm \sqrt{B3^2 - 4.A3.C3}}{2.A3} \quad (31)$$

Depending on the boundary conditions, appropriate sign in Eq. 31 is taken.

where

$$A3 = S2.R2.\sigma_2' - R2.S2.\sigma_1'$$

$$B3 = R8.S2 - S8.R2 + R2.\sigma_1'.S7 - S2.\sigma_2'.R7$$

$$C3 = R7.S8 - S7.R8$$

A first approximation for the co-ordinates of point 3, the point of intersection of characteristics, is obtained from equations (26) and (27). The values of the co-ordinates of point 3 are then used to compute the values of σ_2' and θ_3. A new estimate of the co-ordinates of point 3 is then obtained by taking θ_1 as average of θ at points 1 and 3 and θ_2 as average of θ at points 2 and 3. The new values of σ_3 and θ_3 are thus obtained and the iteration is continued until the values remain essentially unchanged.

(*iv*) *Solution at the slope OA* (see Fig. 1)

As along OA soil moves in the direction of the slope and as normal and shear stresses along it are zero.

$$\theta_{0A} = \pi/ + \beta_o \tag{32}$$

If σ_n is the effective stress along OA in the direction normal to OA, then

$$\sigma_n = \text{total stress in normal direction} - u$$

$$= 0 - u_{0A}$$

$$= -u_{0A}$$

where

u_{0A} = final pore water pressure along OA.

Using

$$\sigma_n = \sigma_{0A}\,(1 - \sin\phi_m.\cos 2\alpha) - H$$

where α = angle of direction of major principle stress with OA measured positive clockwise.

= 0 along OA

Proceeding, as explained before the following expression for σ_{OA} can be obtained

$$\sigma_{OA} = \frac{(U2+1)\,H - U2\,\{u_o\,(K_o-1)\,(1-A) + u_o/B\}}{1+U1-\sin\varphi_m}$$

Dividing by H the non-dimensional equation is

$$\sigma'_{OA} = \frac{(U2-1) - U2\,\{(K_0-1)\,(1-A) + U2/B\}\,u_o/H}{1+U1-\sin\phi_m} \tag{33}$$

(v) Calculation of stability number

The stability number, N_s is defined as

$$N_s = \frac{c}{F.\gamma h}$$

where

c = cohesion of the soil,

F = factor of safety,

h = height of the slope.

Nondimensionalising, N_s can be expressed as

$$N_s = \frac{\tan\phi_m}{h'} \tag{34}$$

Here h' is the non-dimensional depth (Fig. 1) of the ϕ_m contours for which N_s is to be computed. Hence, for different ϕ_m contours, knowing their depth h', at the slope OA, N_s can be calculated.

Method of Solution

A tentative value of ϕ_m is assumed as calculations are started from the top of slope. Computations are carried to the slope and $(\theta+\mu_m)$ line along which ϕ_m is taken to be constant is generated. The value of σ'_{OA} as computed through these computations is compared with the one given by the boundary condition [equation (33)]. If these two values talley within $\pm 10^{-3}$ accuracy, the ϕ_m contour thus developed is accepted else another value of ϕ_m is assumed and the process is repeated. For each contour, N_s is calculated using equation (34).

Results and Discussion

For the assessment of the satisfactory mesh size from the point of view of computer time and accuracy, influence of mesh size on stability number is studied. Fig. 4 shows influence of the spacing of $(\theta+\mu_m)$ line at the top of the slope. It can be seen that for $\triangle x' = 0.2$, the points on the stability curve are not too widely spaced to make a smooth curve through them difficult as they are in the case of $\triangle x' = 0.4$. Also in this case the generation of curve is not excessively slow as in the case of $\triangle x' = 0.1$. It has been found that number of radial lines has very little influence on the stability numbers. In the present analysis $\triangle x' = 0.2$ has been used as spacing and the θ difference between successive radial lines is taken to be less than or equal to 5°.

Numerical results obtained are presented in the form of stability charts.

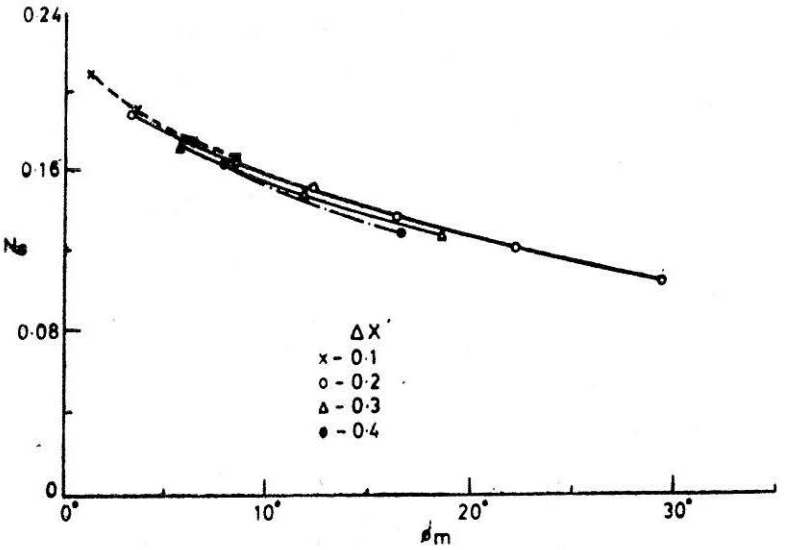

FIGURE 4 Influence of mesh size on N_s for A = B = 0.5, $u_o/H = -0.25$ and $\beta_o = 5°$

For particular set of values of parameters A, B, u_o/H, and β_o, a relationship between N_s and ϕ_m is obtained. This is done for various values of β_o. The value of K_y throughout the analysis is taken as 0.4. Results are discussed in the following three headings.

(*i*) Comparison with the values for $A = B = u_o/H = 0$ from the present analysis

$A = B = u_o/H = 0$ are used to obtain the values of N_s and ϕ_m for dry soil. It can be seen from the Tables 1 & 2 that even for such a small value of u_o/H as —0.25 and $A = B = 0.2$, the decrease in N_s from the one for dry soil ranges from about 5% to 25% depending upon the values of ϕ_m. Therefore, even a small initial negative pore water pressure results in considerable increase in the factor of safety. Table 2 shows a comparison of the values for $A = B = u_o/H = 0$ from the present analysis with the Taylor's (1937) values.

(*ii*) Influence of various parameters on ϕ_m contours

Figs. 5 and 6 show the influence of pore pressure parameters A and B on the ϕ_m contours. It can be seen from these figures that as the value of either A or B increases, everything else remaining constant, the contours of ϕ_m starting from the same point at the top of the slope become shallower and more curved. Also the value of angle of internal friction mobilized along the contour starting from any specific point at the top decreases with increase of either A or B. Just reverse to this is the effect of increasing

TABLE 1

Comparison between the stability numbers for A=B= 0, $u_o/H=0$ with the values from the present analysis for A = B = 0.2, u_o/H = —0.25 and K_o = 0.4

ϕ_m FOR	N_s	β_o=10°	% diff.	β_o=20°	% diff.	β_o=30°	% diff.	β_o=40°	%diff.
1	2	3	4	5	6	7	8	9	10
5°	P*	.206	19.9	.172	20.93	.148	27.02	.126	27.7
	T	.165		.136		.108		.091	
10°	P	.171	18.12	.146	23.09	.116	25.01	.094	24.26
	T	.14		.112		.087		.071	
15°	P	.151	20.52	.118	22.03	.094	27.76	.064	15.62
	T	.12		.092		.068		.054	
20°	P	.133	22.5	.104	25.95	.072	20.83	.042	4.76
	T	.103		.077		.057		.04	
25°	P	.114	25.4	.087	28.73	.056	28.57	.028	10.71
	T	.085		.062		.04		.025	

$P = N_s$ for $A = B = K_o = u_o/H = 0$ case

$T = N_s$ for $A = B = 0.2$, $u_o/H = 0.25$, $K_o = 0.4$

% diff. = Percent decrement in the T values from P values.

TABLE 2

Comparison between Taylor's stability numbers with the values from the present analysis for A = B = u_o/H = 0

ϕ_m	N_s FOR	β_o=10°	% diff.	β_o=20°	% diff.	β_o=30°	% diff.	β_o=40°	% diff.
1	2	3	4	5	6	7	8	9	10
5°	P*	.206	3.28	.172	4.9	.148	8.07	.126	9.35
	T*	.213		.181		.161		.139	
10°	P	.171	7.06	.146	9.8	.116	13.43	.094	21
	T	.184		.162		.134		.119	
15°	P	.151	9.58	.118	11.27	.094	21.0	.064	30.43
	T	.167		.133		.119		.092	
20°	P	.133	10.73	.104	14.04	.074	22.58	.042	39.13
	T	.149		.121		.093		.069	
25°	P	.114	12.3	.087	16.34	.056	26.3	.028	45.0
	T	.13		.104		.076		.051	

*P = Present Analysis

T = Taylors' values

% diff = denotes percent decrement in the values of stability number given by present analysis from those given by Taylor.

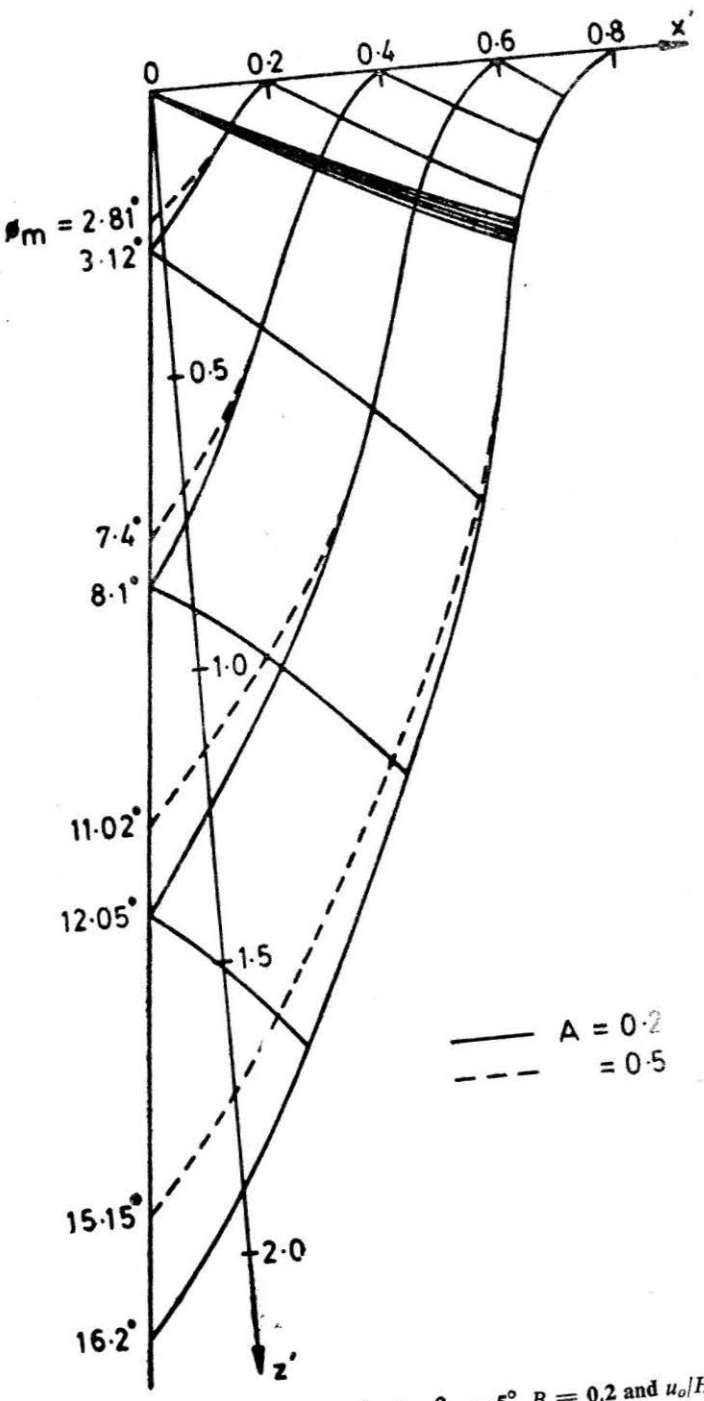

FIGURE 5 Contours of ϕ_m for $\beta_o = 5°$, $B = 0.2$ and $u_o/H = -0.25$

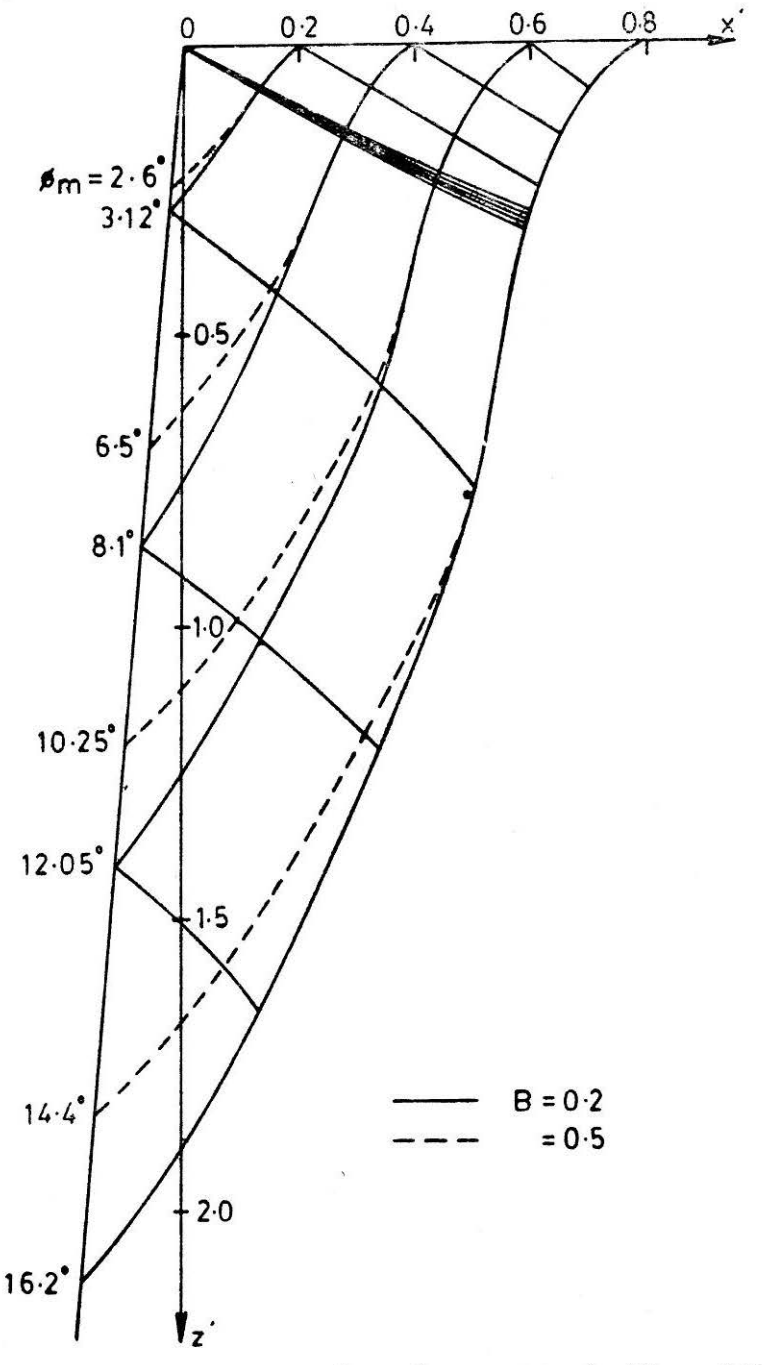

FIGURE 6 Contours of ϕ_m for $\beta_o = 5°$, $A = 0.2$ and $u_o/H = -0.25$

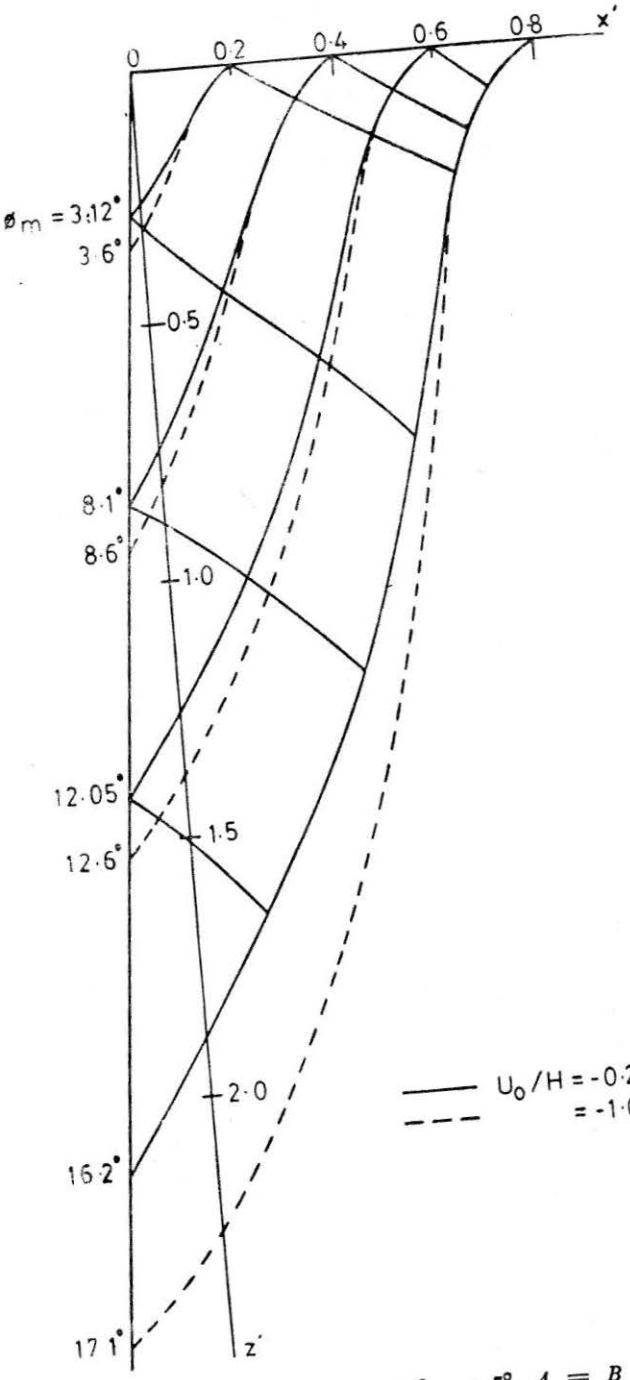

FIGURE 7 Contours of ϕ_m for $\beta_o = 5°$, $A = B = 0.2$

initial suction, u_o/H, on the shape of ϕ_m contours and the value of ϕ mobilized along these contours (Fig. 7). It can be visualized that, when the ϕ of a soil becomes equal to ϕ_m along a certain contour the slope will fail along that characteristic. The points on this characteristic should be in critical equilibrium. Points above it will not be in critical equilibrium.

(*iii*) Influence of various parameters on stability numbers

Figs. 8 to 10 show the stability charts for various values of A, B, u_o/H and β_o. It is found from these charts that for specific values of ϕ_m, β_o and u_o/H, the stability number increases with increase in pore pressure parameters A and B. This can be expected because with increase in parameters B and A, at the same pore water pressure, the pore water pressure goes up thereby decreasing the shear strength of the soil. Contrary to this, the shear strength of the soil improves with increasing values of initial negative pore water pressure, because of enhanced level of effective stress.

Illustrative Example

To illustrate the utility of the results presented the following numerical example is given

Example : Determine the factor of safety of the embankment with partly saturated soil and compare the result [with the result obtained without taking the negative pore water pressure into account for the following data

Height of embankment=10 m,

cohesion of soil, $c = 10$ t/m^2,

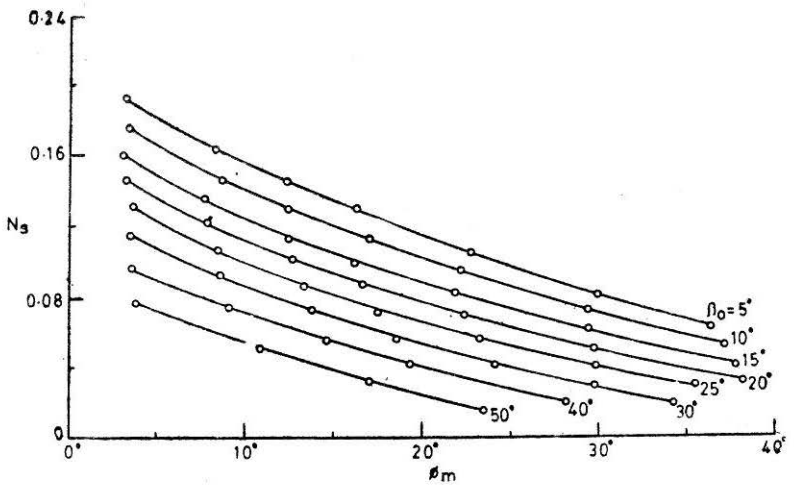

FIGURE 8 Stability chart for $A = B = 0.2$ and $u_o/H = -0.25$

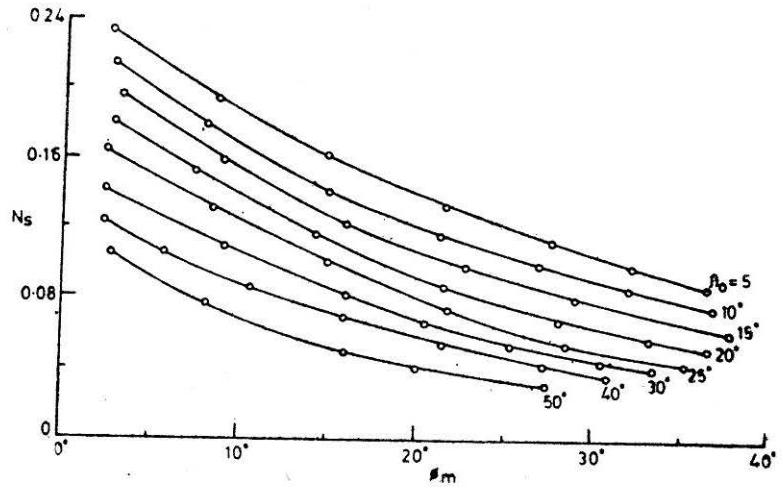

FIGURE 9 Stability chart for $A = 1.0$, $B = 0.7$ and $u_o/H = -0.25$

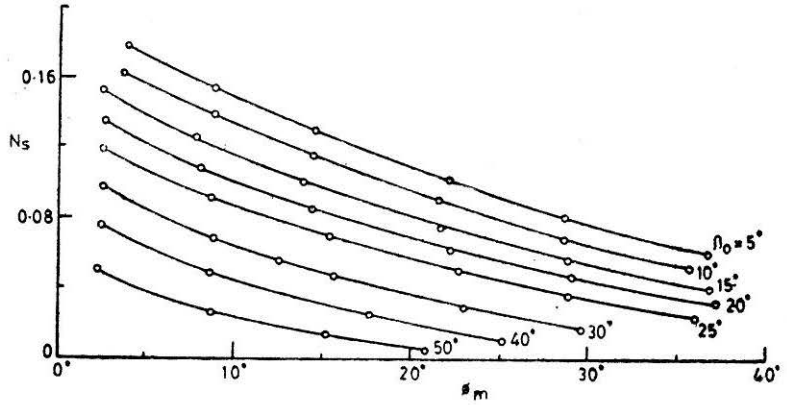

FIGURE 10 Stability chart for $A = B = 0.2$ and $u_o/H = -2.0$

initial pore water pressure $u_o = -14.0$ t/m²

Skempton's pore water pressure parameters, $A=0.2$, $B=0.2$,

angle of internal friction, $\phi = 10°$,

$\gamma = 1.8\ t/m^3$ and $\beta=20°$

$H = c \cot \phi = 13.74\ t/m^3$,

Nondimensional initial pore pressure $\dfrac{u_o}{c \cot\phi} = \dfrac{-14.0}{10 \cot 10} = -0.247$

Case 1 :

Taking into account the negative pore water pressure for $u_o/H = -0.25$, $A = 0.2$, $B = 0.2$, $N_s = 0.165$ (vide Table 1)

Case 2 :

Without taking into account of negative pore water pressure $u_o/H = 0.0$, $A = 0.0$, $B = 0.0$, $N_s = 0.206$ (vide Table 1)

For case 1

$$N_s = \frac{c}{\gamma \times h \times \text{Factor of safety}}$$

$$F.S. = \frac{10}{1.8 \times 10 \times 0.165} = 3.36$$

For case 2

$$\therefore \text{ Factor of safety} = \frac{c}{\gamma \times h \times 0.206} = \frac{10}{1.8 \times 20 \times 0.206} = 2.7$$

The numerical example shows that negative pore water pressure has considerable influence on stability.

Summary and Conclusions

A new approach for the method of characteristics for stability analysis of slopes is presented. The derivation of characteristic equations for the analysis in partially saturated soils is done. No assumption regarding failure surfaces is made. The usual assumption of method of characteristics that the soil is at critical equilibrium at each and every point is deleted. The contours of angle of internal friction mobilized are arrived and presented. Results are given in the form of stability charts. Numerical results presented show that the effect of decrease in pore water pressure parameter and increase in the initial suction level is to improve the shear strength and hence give lesser values of stability numbers or greater values of factor of safety.

REFERENCES

LOWE, J. (1967). Stability Analysis of Embankments. *Journal of Soil Mechanics and Foundation Engineering Division* ASCE, SM4, 1-33.

MOGALAIH G and RANGANATHAM, B.V. (1972) : "Electrochemical environment and negative pore water pressure in compacted Kaolonite", *Proc. of Symposium on Strength and Deformation Behaviour of Soils*, Mysore Centre of Indian Geotechnical Society, Bangalore, India, : 1-9.

OLSON, R.E. and LANGFELDAR, L.J. (1965) : "Pore Water pressures in unsaturated soils", *Jl. of Soil Mech. and Foundation Engg.* Div., ASCE, 96, SM6 : 2171-2180.

REDDY, A.S. and MOGALIAH, G. (1970). Bearing capacity of Partially Saturated Soils. *Journal of Soil Mechanics and Foundation Engineering*. ASCE, 96, SM6, 2175-2180.

SKEMPTON, A.W. (1954). The Pore Pressure Coefficients A and B. *Geotechnique* 4, 145-147.

SOKOLOVSKY, V.V. (1960). Statics of Soil Media. Butterworths Scientific Publications, London.

TAYLOR, D.W. (1937). Stability of Earth Slopes. *Journal of Boston Society of Civil Engineers*, Vol. 24, No. 3, 337-386.

Notations

A, B	Skempton's pore water pressure parameters
c	cohesion of the soil
c_m	mobilized cohesion
K_o	coefficient of earth pressure at rest
u_o	initial negative pore water pressure
u_o/H	non-dimensional value of u_o
x, z	Cartesian coordinates
β_o	slope angle from vertical
θ	angle between the x-axis and the direction of major principal stress, measured positive in the clockwise direction
ϕ	angle of internal friction of the soil
ϕ_m	mobilized angle of internal friction of soil